Resting Cerebral Blood Flow Alterations in Chronic Traumatic Brain Injury: An Arterial Spin Labeling Perfusion fMRI Study

Junghoon Kim,[1] John Whyte,[1] Sunil Patel,[1] Brian Avants,[3,4] Eduardo Europa,[1] Jiongjiong Wang,[4] John Slattery,[1] James C. Gee,[3,4] H. Branch Coslett,[2,4] and John A. Detre[2,4]

Abstract

Non-invasive measurement of resting state cerebral blood flow (CBF) may reflect alterations of brain structure and function after traumatic brain injury (TBI). However, previous imaging studies of resting state brain in chronic TBI have been limited by several factors, including measurement in relative rather than absolute units, use of crude spatial registration methods, exclusion of subjects with substantial focal lesions, and exposure to ionizing radiation, which limits repeated assessments. This study aimed to overcome those obstacles by measuring absolute CBF with an arterial spin labeling perfusion fMRI technique, and using an image preprocessing protocol that is optimized for brains with mixed diffuse and focal injuries characteristic of moderate and severe TBI. Resting state CBF was quantified in 27 individuals with moderate to severe TBI in the chronic stage, and 22 demographically matched healthy controls. In addition to global CBF reductions in the TBI subjects, more prominent regional hypoperfusion was found in the posterior cingulate cortices, the thalami, and multiple locations in the frontal cortices. Diffuse injury, as assessed by tensor-based morphometry, was mainly associated with reduced CBF in the posterior cingulate cortices and the thalami, where the greatest volume losses were detected. Hypoperfusion in superior and middle frontal cortices, in contrast, was associated with focal lesions. These results suggest that structural lesions, both focal and diffuse, are the main contributors to the absolute CBF alterations seen in chronic TBI, and that CBF may serve as a tool to assess functioning neuronal volume. We also speculate that resting reductions in posterior cingulate perfusion may reflect alterations in the default-mode network, and may contribute to the attentional deficits common in TBI.

Key words: arterial spin labeling; cerebral blood flow; lesion; magnetic resonance imaging; traumatic brain injury

Introduction

Each year, approximately 1.5 million people sustain traumatic brain injury (TBI) in the United States alone (Rutland-Brown et al., 2006). Among these survivors, 80,000–90,000 individuals are left with significant long-term cognitive and motor disabilities (Thurman et al., 1999). Despite the gravity of these impairments, it is well established that many TBI survivors demonstrate significant improvements over months and even years post-injury (Himanen et al., 2006; Lannoo et al., 2001; Millis et al., 2001). Accurately measuring the brain's structural and functional damage, and tracking these changes over time in chronic TBI, are of great importance as potential guides to rehabilitative efforts to influence these biological recovery processes. Recent advances in neuroimaging may greatly contribute to this endeavor by providing an *in vivo* tool to measure and monitor brain structure and function (Strangman et al., 2005).

Despite the promise of *in vivo* neuroimaging, the complex nature of the injury (i.e., diffuse injury with varying amounts of superimposed focal lesions), and its complicated consequences for the structure and function of the brain, have made accurate assessment of the true extent of structural damage after TBI very difficult. In particular, diffuse axonal injury and atrophy have frequently been underestimated by the typical structural imaging methods used clinically. In addition, dysfunction of structurally preserved neural systems, as may occur for example in diaschisis, can contribute to cognitive

and motor impairment after TBI, and may, as it resolves, underlie some of the behavioral recovery seen.

Many neuroimaging indices have been proposed for measuring neural damage caused by TBI (for a review, see Anderson et al., 2005). For example, ^{1}H magnetic resonance spectroscopy quantifies N-acetylaspartate and choline that can indicate local cell damage or loss. Positron emission tomography (PET) with [55]Co tracer provides indications of areas of cell death by measuring calcium. Cerebral blood flow (CBF), typically measured by [15]O PET, or more recently by perfusion functional magnetic resonance imaging (fMRI), although not a direct indicator of neural damage, might serve as an indirect index of structural and/or functional alterations of the brain. For example, decreased CBF in grossly preserved areas may indicate reduced neural activity or decreased neuronal volume in such regions. Evidence for this notion comes from the experiments establishing the relationship between local neural activity and CBF (Ances et al., 2000; Ngai et al., 1988), and also the studies illustrating reduced CBF at or near the damaged region (Hattori et al., 2003; Kochanek et al., 2002). However, the interpretation of hyper- or hypoperfusion should be done cautiously in relation to cerebral oxygen consumption to confirm a pathological condition in an individual (Werner and Engelhard, 2007).

Resting CBF may also serve as an indicator for the mechanism underlying cognitive impairment, and for understanding corresponding recovery. Resting perfusion, which is less confounded by differences in behavioral performance between individuals or over time (the "performance confound"), is likely to be a less noisy measure of pathology and biological recovery than task-related relative changes in blood flow, such as those assessed in task-evoked fMRI paradigms. Moreover, measurement of absolute regional blood flow at rest allows direct assessment of the magnitude of blood flow changes occurring with drug treatment or other interventions. It also helps researchers to properly interpret TBI survivors' altered hemodynamic modulations in task-evoked paradigms (Perlstein et al., 2004; Ricker et al., 2001; Sanchez-Carrion et al., 2008), by providing the absolute baseline as reference. In fact, a growing number of studies measuring CBF or functional connectivity suggest that brain activity in the resting state is clinically informative in various neurological populations (Greicius et al., 2004; Kim et al., 2009; Kogure et al., 2000; Rombouts et al., 2005; Vanhaudenhuyse et al., 2010).

The existing literature suggests that measures of cerebral blood flow and metabolism in chronic TBI may provide additional information to that obtained with conventional MRI in terms of both structure and function. Earlier SPECT studies in chronic TBI have reported significantly lowered CBF, mainly in the frontal and temporal areas, and related these alterations to concurrent cognitive dysfunction (Goldenberg et al., 1992; Ichise et al., 1994; Oder et al., 1992; Prayer et al., 1993). More recently, Stamatakis and colleagues (2002), largely confirming these findings in a whole-brain statistical parametric mapping study, provided a comprehensive spatial distribution of CBF abnormalities associated with focal and diffuse TBI. It was reported that the frontal, temporal, and cingulate areas were associated with focal lesions, and that these same areas and the thalamus were related to diffuse injury.

Despite the progress the previous research has achieved, there are many issues that need to be resolved before measures of resting CBF can be widely utilized. These issues include lack of measurement in absolute units, crude spatial registration methods (spatial registration is the alignment of one image with another image), and exposure to ionizing radiation (for detailed accounts of these issues, see the discussion section). In the current study we attempted to overcome these obstacles in several ways. First, we aimed to quantify the absolute regional CBF alterations seen in chronic TBI utilizing a continuous arterial spin labeling (ASL) perfusion fMRI technique we validated in our previous research (Kim et al., 2006; Rao et al., 2007; Troiani et al., 2008; Wang et al., 2005). Using labeled water as an endogenous marker, this method allows us to provide highly reliable measures of absolute CBF without exposure to radiation (Detre and Wang, 2002; Wolf and Detre, 2007). Second, in conducting a whole-brain analysis, we aimed to assess the effects of focal and diffuse lesions on regional CBF by employing an image analysis protocol optimized for handling focal and diffuse injuries. For example, taking advantage of a large transformation image registration technique (Avants et al., 2008), we studied the CBF alterations, even in brains with a substantial degree of atrophy. Our tensor-based morphometry protocol (morphometry is the evaluation of the variation and change in the size and shape of parts of the brain; Kim et al., 2008) enabled us to examine the relationship between local atrophy and CBF level. For brains with focal lesions, we used a variation of cost-function masking (cost function is a mathematical measure of mismatch between two images; Brett et al., 2001) to minimize distortion of lesion locations during the high-dimensional spatial normalization processes. The extent of focal lesions was also delineated thoroughly to examine the local relationship between focal lesions and CBF alterations. Using these methods, the current study aimed to provide a more reliable picture of resting CBF alterations in chronic TBI, and to better differentiate the contributions of focal and diffuse lesions to hypoperfusion.

Methods

Participants

The data were collected as part of a larger study investigating the neural correlates of attention deficits and treatment responses to various psychoactive drugs in the survivors of TBI (principal investigator: J. Whyte). TBI participants were recruited from a variety of clinical services at the Moss Rehabilitation Research Institute, and through a consent-based registry (Schwartz et al., 2005) of individuals with TBI who are interested in participating in rehabilitation research. To be included, participants had to be between the ages of 16 and 60 years, and had to have a history of non-penetrating TBI of at least moderate severity at least 3 months prior to enrollment. Severity level was defined by significant and well-documented loss or alteration of consciousness following injury (i.e., lowest Glasgow Coma Scale [GCS] score of < 12, or prospectively documented post-traumatic amnesia [PTA] of > 1 h), or focal abnormality on a neuroimaging study that was attributable to traumatic injury. Because these data were collected as part of a larger project on the treatment of attention deficits, self- or clinician-reported attention complaints were also required. Potential participants were excluded if they had a history of pre-morbid neurological disease, psychosis, major affective disorder, developmental disability, or attention deficit-hyperactivity disorder, or if they were currently abusing alcohol or recreational drugs. Persons who

were taking psychoactive medications other than anticonvulsants were also excluded. Participants and/or their involved caregivers (depending on the participant's cognitive capacity) provided informed consent. The study protocol was approved by the Albert Einstein Healthcare Network and the University of Pennsylvania institutional research boards. Twenty-two healthy volunteers, matched to patients for age, gender, handedness, years of education, and ethnicity, were recruited based on the same inclusion/exclusion criteria as the patients, with the exception that they never had a TBI resulting in loss or alteration of consciousness, or suffered attention complaints. Control participants were recruited through the family and friendship networks of the participants with TBI, and through public advertising.

Among the 32 TBI survivors recruited, one was excluded due to a large (filling the entire right hemisphere) lesion. Two individuals with TBI were excluded due to excessive movements during scanning (defined in the image analysis section), and another two due to limited brain coverage after spatial normalization. Twenty-three healthy control participants were initially recruited, and one of them was excluded due to excessive motion. As a result, data from 27 individuals with TBI and 22 healthy volunteers were included in the final analysis of the current study. Structural MRI scans from a subset of these individuals, who were recruited earlier, were used in our previous morphometry study (Kim et al., 2008). Tables 1 and 2 show selected demographic and clinical characteristics of the participants included in the final analysis of the current study. Overall, the patients did not differ significantly from healthy controls in terms of age, gender, ethnicity, handedness, or years of education. In addition, the two patient subgroups (focal and diffuse; see the subgroup analysis in the results section) did not differ from controls or from each other on any measures (as tested with t-test or Fisher's exact test, as appropriate; all p values > 0.1), except total lesion volume ($p < 0.001$). Measures of the functional status of each participant at the time of testing were not obtained prospectively. However, patients were retrospectively assigned Glasgow Outcome Scores (GOS; Jennett et al., 1981), based on a review of referral records and observation of the participants at testing. Because we lacked information about current employment status in many cases, these ratings remain somewhat imprecise, indicating the lowest possible level of function compatible with the available data at the time of testing. Out of 27 patients, 11 were rated as level 3 (severely disabled) or better; 11 were rated as level 4 or better (moderate disability); and 5 were rated as level 5 (good recovery).

Imaging data acquisition

The structural and functional imaging was conducted on a Siemens 3.0 T Trio whole-body scanner (Siemens AG, Erlangen, Germany), using a standard transmit/receive head coil. The resting perfusion scan reported in this study was obtained in the middle of four (or five) cognitive task scans, the results of which will be reported in separate articles. Before the functional scans were done, high-resolution T1-weighted anatomic images were obtained using a 3D MPRAGE sequence ($1 \, mm^3$ resolution). For perfusion fMRI scans, an amplitude-modulated continuous ASL (CASL) technique was implemented (Wang et al., 2005). Interleaved images with and without labeling were acquired using a gradient echo echo-planar imaging sequence with the following acquisition parameters: FOV = 22 cm; matrix = 64×64; TR = 4 sec; TE = 17 msec; flip angle = 90°). Fourteen slices (6 mm thick with a 1.5 mm gap) were acquired to cover the whole brain. For detailed imaging parameters, refer to our previous publication (Kim et al., 2006). During a 6-min scan (92 acquisitions), the participants were asked to close their eyes but stay awake.

Image analysis

Delineation of focal lesions. The precise location and extent of focal lesions was assessed for better interpretation of the CBF results in the presence of such lesions. Focal lesions included any cystic cavities and other focal regions of abnormal signal in the white or gray matter. Fourteen out of 27 TBI survivors showed detectable focal lesions (Tables 1 and 2). For more technical details, see our previous study (Kim et al., 2008).

Spatial normalization and tensor-based morphometry. A custom template representing the average of the brain images of both controls and TBI patients was built. Symmetrical normalization (SyN; Avants and Gee, 2004; Avants et al., 2008) was used to register brains to the template. For the brains with focal lesions (defined as those with a total lesion volume $> 1 \, cm^3$), a variation of the cost-function masking method (Brett et al., 2001) was used in combination with SyN. In essence, this method allows transformation in the lesioned area to be "constrained," while intact areas go through a large degree of transformation. As a result of spatial transformations, we were able to obtain Jacobian values that indicate volume expansion and contraction at each location of the brain. For a detailed description of the procedure of tensor-based morphometry, refer to our previous publication (Kim et al., 2008).

TABLE 1. SELECTED DEMOGRAPHIC AND CLINICAL CHARACTERISTICS OF HEALTHY CONTROLS AND TBI SURVIVORS

	Controls	TBI (all patients)	TBI (focal subgroup)	TBI (diffuse subgroup)
Number	22	27	12	15
Male/female	19/3	21/6	10/2	11/4
Age (y)	32.7 ± 9.9	36.7 ± 12.3	39.0 ± 14.4	35.6 ± 10.6
Ethnicity (C/AA/H/A)	11/7/0/3	13/9/4/1	6/4/2/0	7/5/2/1
Handedness (right/left)	19/3	23/4	10/2	13/2
Education (years)	13.2 ± 1.9	13.2 ± 2.7	12.8 ± 2.4	13.7 ± 2.8
Months post-injury	NA	65.7 ± 82.2	77.5 ± 94.5	57.1 ± 72.9
Total lesion volume (cm³)	NA	26.1 ± 46.9	58.5 ± 55.9	0.1 ± 0.3

Numbers after ± are standard deviations
C, Caucasian; AA, African-American; H, Hispanic; A, Asian; TBI, traumatic brain injury.

TABLE 2. SELECTED CLINICAL CHARACTERISTICS OF TBI SURVIVORS

Patient ID	Age	Gender	Months post-injury	Cause of TBI	Lesion location at the time of testing	Total lesion volume (cm³)
Focal subgroup						
3	47.9	M	67.1	MVA	L temporal pole; R occipital	43.8
4	46.0	M	330.2	MVA	R temporal and orbitofrontal	32.4
7	48.7	M	121.9	Assault	L superior temporal and orbitofrontal; L superior frontal	9.9
9	23.3	M	78.0	MVA	L frontal pole and orbitofrontal lesion extending to superior frontal	64.5
10	18.8	M	16.5	Fall	R temporal pole; R orbitofrontal; L orbitofrontal	87.7
12	22.9	M	16.2	Car/ped	R temporal pole; L superior frontal	23.7
19	30.0	M	160.3	MVA	L subcortical lesion involving thalamus, basal ganglia, and internal/external capsule extending into centrum semiovale	17.1
22	56.2	M	15.0	Fall	Bilateral orbitofrontal extending into frontal pole superiorly	113.3
27	47.2	M	95.5	Assault	L frontal lesion extending into anterior temporal; L superior temporal; R temporal, occipital, and parietal cortices	203.3
28	53.4	F	7.4	Fall	L superior frontal; L temporal; R internal capsule; R putamen; L thalamus	2.3
31	21.6	F	8.2	MVA	L temporal and bilateral superior frontal; R putamen	43.6
33	52.3	M	13.6	MVA	Bilateral prefrontal	60.2
Diffuse subgroup						
1	25.7	M	31.6	NK		
5	31.3	M	72.1	MVA	R superior frontal	0.7
8	42.4	F	224.6	MVA		
11	38.4	M	184.4	MVA		
14	42.7	M	18.6	MVA		
15	23.1	M	47.1	MVA	R thalamus	0.2
16	58.4	F	160.8	MVA		
17	42.5	M	8.1	Assault		
18	23.9	F	6.4	NK	R superior frontal; posterior body of CC	0.9
21	24.7	M	4.1	Car/ped		
23	43.9	M	4.8	MVA		
24	24.6	M	25.3	MVA		
26	33.1	F	4.5	MVA		
29	43.0	M	7.2	Car/bike		
34	24.3	M	44.7	MVA		

M, male; F, female; MVA, motor vehicle accident; Car/ped, car/pedestrian accident; Car/bike, Car/bike accident; NK, not known; R, right; L, left; TBI, traumatic brain injury; CC, corpus callosum.

Functional image processing. A perfusion-weighted image series was generated by the procedures described in our previous publications (Kim et al., 2006; Wang et al., 2005). Movement parameters were extracted using the SPM2 realign algorithm. If the average of maximal translational displacements along three axes (x, y, and z) during a session exceeded the average of voxel dimensions along three axes, it was regarded as excessive motion. On this basis, the data from two patients were discarded.

In our map-wise analysis, we report only clusters satisfying a combinatory criterion of a peak height threshold of $p < 0.001$, and a cluster size threshold of $k > 50$. For the group comparisons involving all subjects (i.e., 27 TBI survivors and 22 controls), this threshold yields a whole-brain false-discovery rate (FDR) of less than 5% after correction for multiple comparisons. However, due to reduced statistical power, no voxels survived the FDR 5% threshold in some subgroup analyses. In

any case, we provide FDR-corrected p values for the identified voxel clusters reported in the tables. The anatomical labels of the peaks in the custom template were manually obtained using a human atlas of neuroanatomy (Mai et al., 2004). To calculate the mean CBF differences (ΔCBF) between two groups (or subgroups) reported in the tables, the CBF time series for each voxel from each subject was averaged across all the voxels in each significant voxel cluster, and then averaged across subjects. For the analysis of relative CBF, a proportional scaling method implemented in SPM5 was used to globally normalize each subject's absolute CBF images.

Biological parametric mapping (BPM)

The BPM analysis was developed to combine information from multiple imaging modalities (Casanova et al., 2007). This allows one to build a unique statistical model at each location
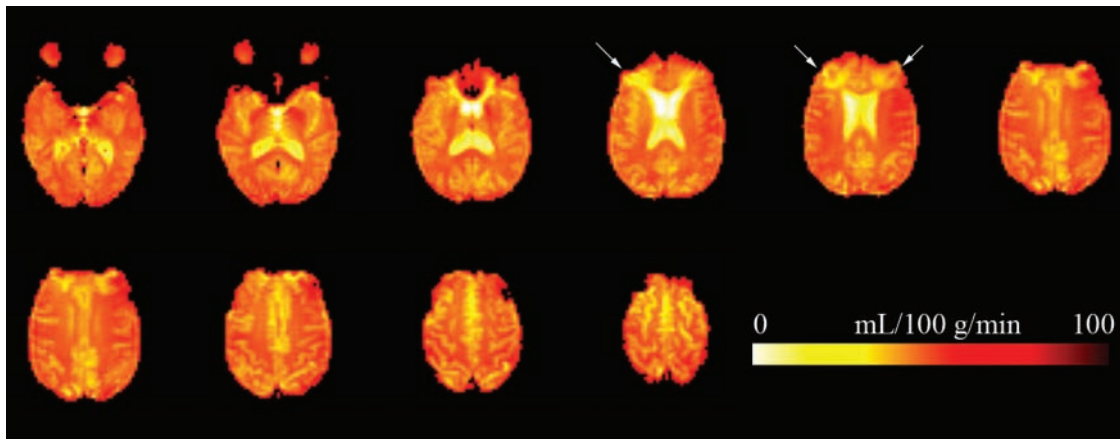
FIG. 1. Mean raw cerebral blood flow images in an individual with traumatic brain injury. Total acquisition time was approximately 6 min. The patient had bilateral orbitofrontal lesions extending into the frontal pole superiorly (white arrows). (Color image is available online at www.liebertonline.com/neu)

of the brain. The current study used this technique to investigate: (1) the relationship between CBF and gross volume change as quantified by tensor-based morphometry, and (2) group differences in CBF after accounting for gross volume change (i.e., atrophy).

Results

Group differences in global absolute CBF

Figure 1 illustrates a patient's raw CBF image. Before conducting local-level map-wise analyses, global absolute CBF in
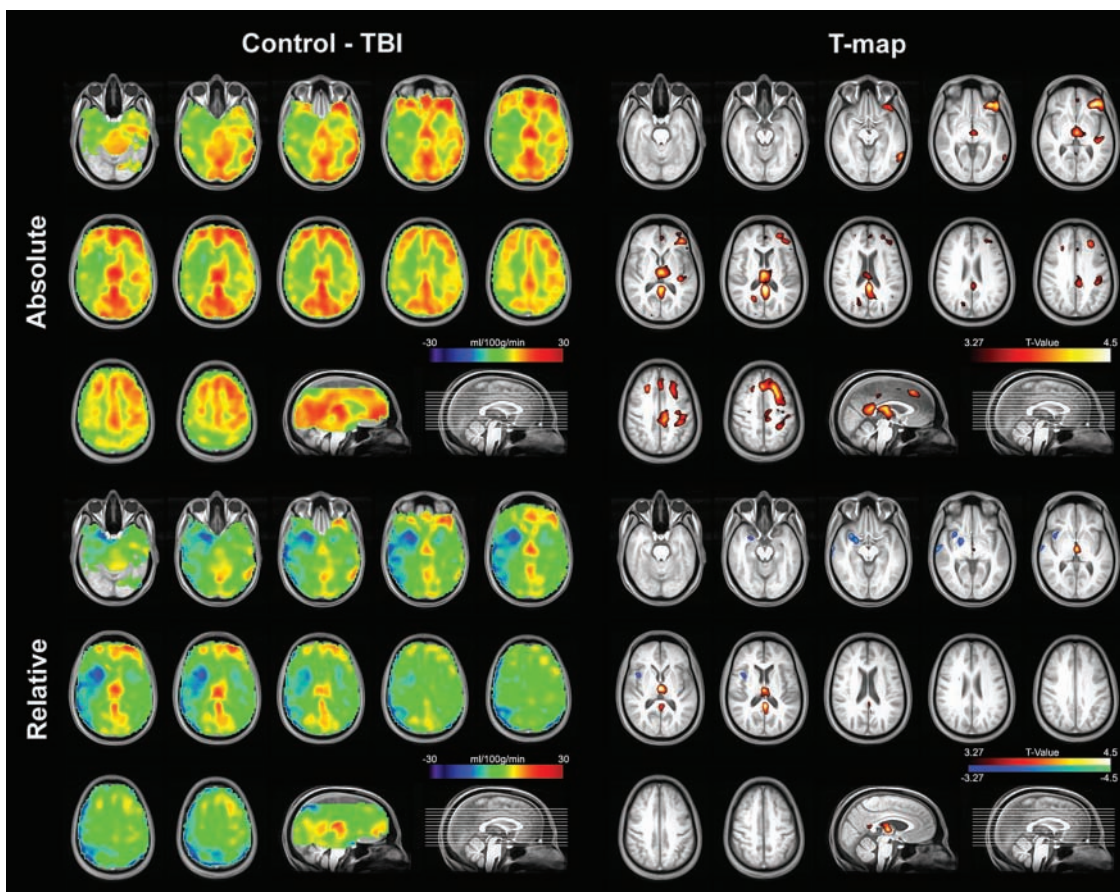
FIG. 2. Top panels: Absolute mean cerebral blood flow (CBF) difference map between control ($n = 22$) and TBI ($n = 27$) groups (left), and the corresponding voxel-wise statistical map, thresholded with a whole-brain false-discovery rate of less than 5% (right). Bottom panels: Relative mean CBF difference map from the same groups (left), and the corresponding statistical map (right). Radiological convention is used. (Color image is available online at www.liebertonline.com/neu)

each group was calculated to confirm that CBF reduction in chronic TBI is detectable at the whole-brain level. As expected, there was a significant difference between the two groups in the segmented whole-brain gray matter (control mean = 56.3 mL/100 g/min; SD = 11.6; patient mean = 48.0 mL/100 g/min; SD = 9.2; independent sample t-test without equal variance assumption, $t = 2.7$, df = 39.7, $p < 0.01$), and white matter (control mean = 42.3 mL/100 g/min; SD = 8.9; patient mean = 35.9 mL/100 g/min; SD = 7.1; $t = 2.8$, df = 39.7, $p < 0.01$). The average CBF value within the focally lesioned areas ($n = 12$; see subgroup analysis section below) was 30.4 mL/100 g/min (SD = 9.8). However, these values should be interpreted with a great deal of caution because the crude gray versus white matter segmentation by SPM5, and smoothing as a step of preprocessing, may confound the values from different tissue types.

Group differences in regional absolute CBF

A whole-brain map resulting from an independent two-sample t-test between 27 TBI survivors and 22 healthy controls is shown in the upper panels of Figure 2. Statistically significant hypoperfusion was found in bilateral posterior cingulate cortices, the left inferior frontal cortex, bilateral thalami, bilateral superior and middle frontal cortices, the left pre- and post-central cortices, the left transverse temporal cortex, the right precuneus, and bilateral anterior cingulate cortices. The top panel of Table 3 shows statistics for the clusters identified as significant. There were no voxels in which patients showed significantly greater CBF than controls.

Group differences in regional relative CBF

Although we believe using absolute CBF is more appropriate in TBI because chronic TBI patients are characterized by widespread hypoperfusion, relative CBF was calculated to compare our data with previous research. Compared to healthy controls, TBI patients showed relative hypoperfusion in bilateral thalami and bilateral posterior cingulate gyri (the middle panel of Table 3 and the upper panels of Fig. 2). However, unlike the results from the absolute CBF data, TBI patients showed a relative increase in CBF compared to controls in a few areas, including the right temporal gyri and the right insula (the bottom panel of Table 3 and the lower panels of Fig. 2).

TABLE 3. REGIONS OF SIGNIFICANT GROUP DIFFERENCE IN ABSOLUTE (UPPER PANEL) AND RELATIVE (LOWER PANEL) CBF BETWEEN 22 HEALTHY CONTROL SUBJECTS AND 27 TBI SURVIVORS

	Size (voxels)		Anatomical label	BA	p (FDR-corrected)	Δ CBF (mL/100 g/min)	% CBF reduction
Absolute CBF				Control - patient			
	879	R	Posterior cingulate gyrus	23/26	0.017	15.2	26.7
		R	Thalamus	NA	0.017		
		R	Thalamus	NA	0.017		
	959	L	Inferior frontal gyrus	47	0.017	14.6	24.9
		L	Superior frontal gyrus	8	0.017		
		L	Middle frontal gyrus	8	0.017		
	70	L	Middle temporal gyrus	37	0.017	16.0	24.4
	61	R	Middle frontal gyrus	9	0.017	12.3	25.8
	216	L	Precentral gyrus	4	0.017	11.7	20.9
		L	Postcentral gyrus	3	0.017		
		L	Postcentral gyrus	3	0.017		
	72	L	Transverse temporal gyrus	41	0.017	11.7	18.0
	62	R	Precuneus	7	0.017	13.4	25.3
		R	Precuneus	31	0.017		
	51	R	Anterior cingulate gyrus	32	0.017	17.0	25.9
		L	Anterior cingulate gyrus	32	0.018		
Relative CBF				Control - patient			
	156	R	Thalamus	NA	0.09	NA	NA
			NA	NA	0.09	NA	NA
	78	R	Posterior cingulate gyrus	23	0.09	NA	NA
				Patient - Control			
	59	R	Middle temporal gyrus	21	0.15	NA	NA
		R	Superior temporal gyrus	22	0.15	NA	NA
		R	Middle temporal gyrus	21	0.157	NA	NA
	176	R	Insula	38/48	0.15	NA	NA
		R	Parahippocampal gyrus	34	0.15	NA	NA
		R	Inferior frontal gyrus	44	0.15	NA	NA

Coordinates of local maxima at least 8 mm apart are reported for each cluster (maximum 3 maxima).
R, right; L, left; BA, Brodmann area; NA, not applicable; CBF, cerebral blood flow; FDR, false-discovery rate; TBI, traumatic brain injury.

Subgroup analysis

In an attempt to differentiate the effects of focal and diffuse lesions on resting CBF, a subgroup analysis was conducted in which 12 TBI survivors with focal lesions (i.e., a total focal lesion volume $>1\,cm^3$) formed the "focal" subgroup, and the remaining 15 subjects formed the "diffuse" subgroup. (This grouping should not be interpreted as a strict dichotomy, because many patients in the focal subgroup demonstrated diffuse lesion characteristics such as atrophy, and three patients in the diffuse subgroup also had small ($<1\,cm^3$) focal lesions.) The main results of subgroup analysis can be summarized as follows. First, as shown in the mean perfusion difference maps (Fig. 3, upper panels), and confirmed by a whole-brain map-wise statistical comparison (Table 4, top and middle panels), both subgroups displayed areas of hypoperfusion compared to controls in bilateral posterior cingulate gyri. Second, as the direct comparison of the focal and diffuse groups shows (Fig. 3, lower left panel), the focal group demonstrated more prominent CBF reductions in frontal areas, particularly in the superior and middle frontal cortices (Table 4, bottom panel). Third, these areas of mean CBF difference between the diffuse and focal subgroups fell within the areas of focal structural lesions, as represented by the lesion frequency map (Fig. 3, lower right panel).

Local relationship between atrophy (diffuse lesion) and CBF

Before conducting a local-level analysis, we first plotted the relationship between the mean global CBF (defined by the average of CBF within gray and white matter combined), and gross brain volume (excluding the ventricles; normalized by each individual's within-skull volume; Fig. 4). A significant correlation between the two measures was observed (Spearman's rho $= .34$, $n = 49$, $p < 0.05$). However, no significant correlations were found within each group, indicating that the observed correlation was largely driven by group differences. Again, these results must be interpreted with caution due to the limited resolution of the CBF images and the crude segmentation.
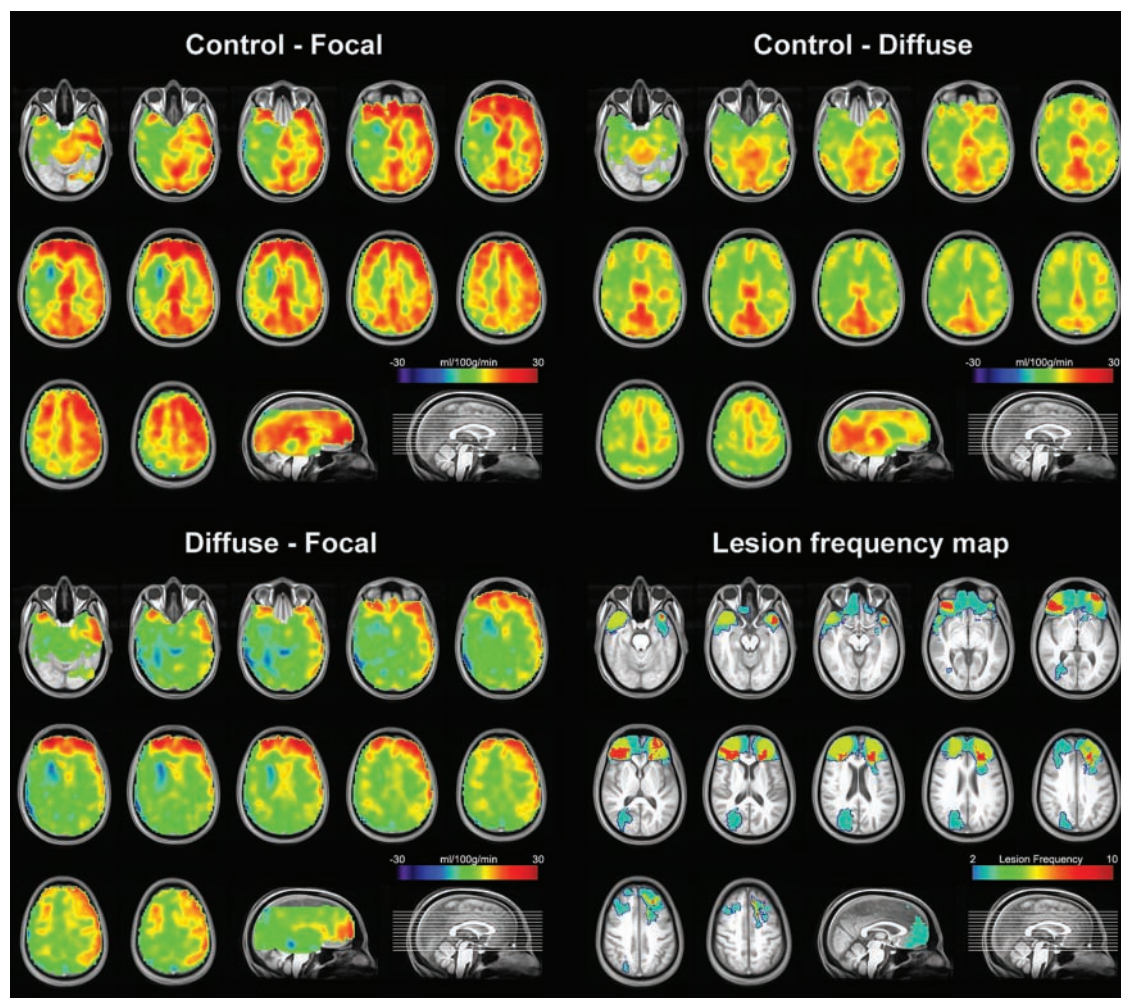
FIG. 3. Top left: Mean cerebral blood flow (CBF) difference map between controls ($n = 22$) and traumatic brain injury (TBI) survivors with focal lesions ($n = 12$). Top right: Difference between controls and TBI survivors without focal lesions (diffuse subgroup, $n = 15$). Bottom left: Mean CBF difference between the diffuse and focal subgroups. Bottom right: Lesion frequency map displaying the 12 TBI survivors with focal lesions. Radiological convention is used. (Color image is available online at www.liebertonline.com/neu)

TABLE 4. REGIONS OF SIGNIFICANT GROUP DIFFERENCE IN ABSOLUTE CBF AMONG THE CONTROL AND THE TBI SUBGROUPS

Size (voxels)		Anatomical Label	BA	p (FDR-corrected)	Δ CBF (mL/100 g/min)	% CBF reduction
Control - focal						
1985	L	Middle frontal gyrus	11	0.009	13.7	24.2
	L	Inferior frontal gyrus	47	0.009		
	L	Inferior frontal gyrus	11/47	0.009		
169	R	Inferior frontal gyrus	47	0.009	13.2	24.9
161	R	Middle frontal gyrus	46	0.009	11.3	23.5
	R	Middle frontal gyrus	6/9	0.011		
	R	Middle frontal gyrus	6	0.012		
86	L	Inferior temporal gyrus	37	0.009	16.0	24.2
368	R	Posterior cingulate gyrus	23/26	0.009	16.3	31.1
	R	Thalamus	NA	0.009		
	R	Thalamus	NA	0.009		
235	L	Middle temporal gyrus	48	0.009	10.9	18.3
	L	Inferior temporal gyrus	20	0.009		
	L	Superior temporal gyrus	22/48	0.012		
51	L	Postcentral gyrus	3	0.009	9.3	15.9
54	L	Precentral gyrus	6	0.009	12.0	21.4
	L	Precentral gyrus	6	0.012		
Control - diffuse						
58	R	Posterior cingulate gyrus	31	0.142	18.8	28.4
Diffuse - focal						
127	L	Middle frontal gyrus	11	0.254	16.2	27.2
	L	Superior frontal gyrus	10	0.254		

Coordinates of local maxima at least 8 mm apart are reported for each cluster (maximum 3 maxima).
R, right; L, left; BA, Brodmann area; NA, not applicable; CBF, cerebral blood flow; TBI, traumatic brain injury; FDR, false-discovery rate.

In order to examine whether there is a local relationship between structural atrophy and cerebral perfusion, the volume loss information quantified by our tensor-based morphometry protocol was correlated with regional perfusion. Specifically, a correlation between the Jacobian determinant value and absolute CBF level was obtained for each voxel using the BPM software. In reporting the results, the areas where more than one patient showed a focal lesion were excluded because the focus of the analysis was the relationship between CBF and diffuse injury. Table 5 (upper panel) shows
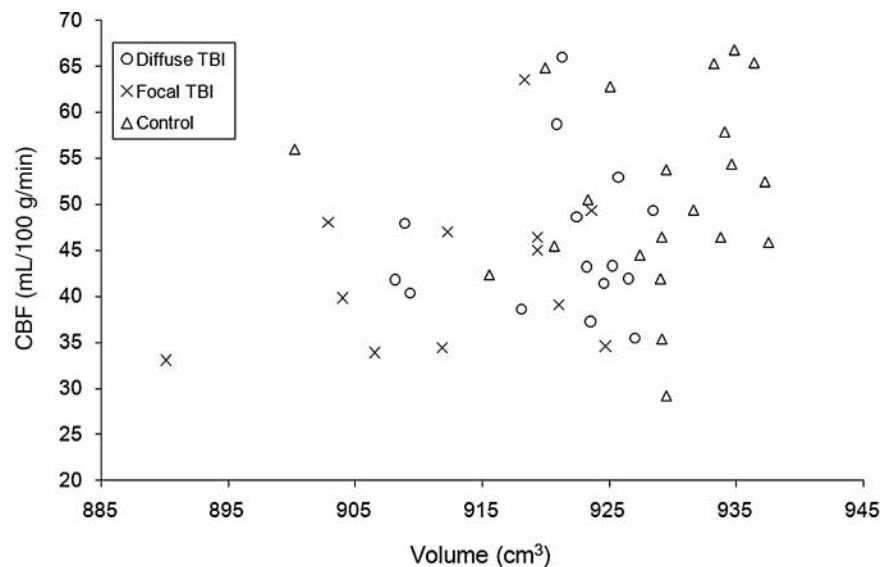

FIG. 4. Relationship between gross volume and cerebral blood flow. Each symbol represents one participant. Individuals with traumatic brain injury (TBI) were divided into two subgroups.

TABLE 5. RELATIONSHIP BETWEEN ATROPHY AND CBF

Size (voxels)		Anatomical label	BA	p (FDR-corrected)
Correlation (all subjects)				
149	L	Thalamus	NA	0.053
	L	Thalamus	NA	0.053
ANCOVA (control - patient)				
129	R	Thalamus	NA	0.024
	R	Thalamus	NA	0.024
	R	Posterior cingulate gyrus	23	0.024
116	R	Precuneus	7	0.024
	R	Precuneus	7	0.024
51	L	Posterior cingulate gyrus	31	0.024
75	L	Precuneus	7	0.024
	L	Precuneus	7	0.024

Regions of significant correlation between diffuse volume changes and CBF (upper panel).

Significant group difference between 22 controls and 27 TBI survivors in absolute CBF after accounting for such volume changes (lower panel).

Coordinates of local maxima at least 8 mm apart are reported for each cluster (maximum 3 maxima).

R, right; L, left; BA, Brodmann area; NA, not applicable; CBF, cerebral blood flow; ANCOVA, analysis of covariance; TBI, traumatic brain injury.

map-wise statistics for the correlation analysis. As shown in the table, the only significant correlations between volume loss and CBF were found in the thalamus.

Encouraged by the relationship between the thalamic atrophy and CBF, we asked the more general question of whether any group differences in absolute CBF (reported in Table 3) would remain after accounting for atrophy. To answer this question, we ran a whole-brain map-wise AN-COVA using the BPM software with CBF value as the dependent variable, and volume change (Jacobian determinant) as a covariate. As shown in the lower panel of Table 5, the thalamus was still identified as a significant cluster after structural adjustment, even though the extent of the cluster was reduced substantially (see Table 3 for comparison).

Discussion

Accurate assessment of true brain damage after TBI must reflect both the structural and functional consequences of the injury. In this regard, it has often been claimed that functional imaging indices such as cerebral perfusion and metabolism may detect brain damage induced by TBI better than conventional CT or MRI scans (Anderson et al., 2005). However, previous studies attempting to map alterations of these functional indices in TBI have suffered from several important limitations. First, most attempts to assess the resting brain state in chronic TBI have used imaging modalities requiring radiation exposure such as PET or SPECT, which are costly and difficult to use in longitudinal research requiring repeated assessments. Thus a validated imaging protocol that does not require radiation exposure would have great utility. Second, a

number of early studies of resting brain activity in TBI used only a region-of-interest (ROI) approach, in which cerebral parameters from a priori global and/or regional ROIs were calculated and compared with those of healthy control participants (for a review, see Azouvi, 2000). However, this approach has been criticized by many authors (Kato et al., 2007; Nakashima et al., 2007; Stamatakis et al., 2002), because of limited spatial resolution, labor intensiveness, poor objectivity, and low reproducibility. Thus, whole-brain mapping studies that can provide a more comprehensive picture of CBF alterations in TBI were warranted.

Third, even the few published whole-brain mapping studies of the resting brain state in TBI (Kato et al., 2007; Nakashima et al., 2007; Stamatakis et al., 2002) without exception employed a "global normalization" procedure (i.e., proportionally scaling the data to the global mean CBF value), thus providing only relative blood flow or metabolism. Recent research suggests that results obtained by analyzing only relative CBF are harder to interpret, and can lead to artifactual findings, especially when there are between-group differences in global mean perfusion (Borghammer et al., 2009a, 2009b; Grunder, 2009). Given the fact that patients with chronic TBI have been reported to demonstrate absolute CBF reductions at a global level (Inoue et al., 2005), delineating the pattern of absolute CBF levels in TBI must be done first to properly interpret relative CBF.

Fourth, a careful analysis of the relationship between patterns of perfusion and patterns of structural damage (both focal and diffuse) has not been done, despite its importance in considering how CBF may inform an understanding of neuropathology and recovery in TBI. This is largely because the brains distorted by diffuse and focal types of pathology have posed a great methodological challenge to whole-brain mapping studies requiring group analysis. For example, spatial registration methods used in previous studies have been either linear or small deformation ("deformation" meaning image transformation), non-linear algorithms that are not adequate for warping brains with a large degree of atrophy, forcing researchers to exclude patients with significant diffuse injury from their analysis. This limitation may have also resulted in poorly aligned functional images across subjects who were included, reducing statistical sensitivity and increasing false-negative findings. As for brains with focal lesions, spatial registration algorithms are required that introduce minimal distortion of lesioned areas, because most spatial normalization processes can be influenced by areas of signal alteration (i.e., encephalomalacia or contusion), that are not present in the standard template. It is also desirable that the extent of such lesions be delineated in detail and compared to the topography of CBF. Many recent whole-brain mapping studies in TBI either did not quantitatively describe the extent of focal lesions, or employed rather loose thresholds (10 or even 25 cm^3) of total lesion volume for excluding focally lesioned brains, consequently including significant numbers of focal lesions in their "diffuse" TBI group (Chiu Wong et al., 2006; Kato et al., 2007; Nakashima et al., 2007; Stamatakis et al., 2002). Reflecting these issues, previous mapping studies of the resting state in TBI have yielded inconsistent patterns. One noticeable inconsistency is between the results from the FDG-PET (Kato et al., 2007; Nakashima et al., 2007) and SPECT studies (Shin et al., 2006; Stamatakis et al., 2002). While both types of studies reported hypo-metabolism or hypo-perfusion

in the anterior cingulate, hypo-metabolism in posterior cingulate areas was reported only in the PET studies.

We used noninvasive perfusion fMRI to provide a more definite picture of resting CBF alterations in individuals with chronic TBI. Utilizing an image analysis protocol optimized for handling brains with focal and diffuse lesions, we also examined the relationship between these alterations and focal/diffuse structural lesions. Our main findings are discussed below.

First, global hypoperfusion was detectable in the brains of participants with TBI, with disproportionate CBF reductions seen in the posterior cingulate cortices, the thalami, and many locations in the frontal cortices. These results suggest widespread but non-uniform hypoperfusion. Whether there are any brain regions with completely normal perfusion is difficult to determine in this relatively small sample.

Second, results from relative CBF data were largely in agreement with the absolute CBF results, except that the TBI patients showed a relative increase of CBF in a few areas, including the right anterior temporal and inferior frontal cortices, compared to controls. Given the fact that there were no actual increases in absolute perfusion in patients compared to controls in the same regions (Fig. 2, upper left panel), this result is likely to be an artifactual finding, in which areas with relatively preserved perfusion in patients turned into "hyperperfused" regions after adjusting for the overall hypoperfusion seen in the patients (Borghammer et al., 2009a, 2009b; Grunder, 2009). More broadly, this suggests that standardizing perfusion measures to individuals' whole-brain perfusion is an unwise practice in TBI research, as it may lead to spurious findings.

Third, focal and diffuse lesion types affected cerebral perfusion in different ways and in different locations. The diffuse subgroup showed areas of hypoperfusion in the bilateral posterior cingulate gyri, indicating that CBF alterations in these areas are related to diffuse pathology. In fact, however, the focal group also showed hypoperfusion in the same areas, indicating that the "focal" group is more accurately described as a diffusely-injured group with superimposed focal lesions. These interpretations were further supported by a direct comparison between the two groups. There were no significant differences between the two groups in the posterior cingulate cortex (Table 4; also see the lower left panel of Fig. 3). Our results are more in agreement with previous PET studies (Kato et al., 2007; Nakashima et al., 2007) than SPECT studies (Shin et al., 2006; Stamatakis et al., 2002), in that we found resting-state alterations in the posterior cingulate cortices and the thalami. It is difficult to explain the discrepant findings across studies with certainty, because there are numerous methodological differences among them. Nevertheless, we speculate that the lack of hypoperfusion in the posterior cingulate cortex in the previous SPECT studies might be explained by their using the low-dimensional spatial normalization (e.g., affine-only), because the effects of misalignment of normalized individual images tend to be greater around the ventricles, due to spatial smoothing and partial volume effects. If hypoperfusion in the posterior cingulate cortices is replicated in future studies, this may mean that the diffuse pathology of TBI involves alterations of the "default-mode" network, in which the posterior cingulate areas play a central role (Fransson and Marrelec, 2008). Given the recent evidence suggesting that failure to appropriately modulate the default-mode network can lead to attention deficits (Kelly et al., 2008; Weissman et al., 2006), we speculate that the hypoperfusion in the posterior cingulate cortex may be implicated in cognitive deficits in TBI survivors.

Fourth, the degree of diffuse volume loss in the thalamus showed a relationship with CBF in the same region. In other words, atrophied thalami had more reduced blood flow, even on a per-volume basis. This local effect of diffuse structural pathology seems to contradict the findings of Nakashima and colleagues (2007). They speculated that the decreased cerebral metabolism observed in the cingulate, lingual, and cuneus cortices of TBI patients in their study was a remote result of deafferentation, rather than the consequence of local neuronal loss or damage, because they did not find significant atrophy in those areas. It is quite possible that more sensitive measurement of tissue loss would have revealed an association that might have explained, at least in part, the hypoperfusion seen in those areas. We propose that CBF measured by perfusion fMRI may serve as a tool to assess functioning neuronal volume in a given structure. In agreement with the notion that actual tissue loss or damage is present in the thalamus, recent evidence from animal studies identified atrophy in thalamic neurons (Lifshitz et al., 2007).

Diffuse and focal injuries may be associated with regional CBF changes through various physiological mechanisms. To date, the lack of validated tools has prevented researchers from differentiating those mechanisms using neuroimaging. With the development of new imaging modalities such as DTI, and better analysis protocols in lesion delineation and spatial registration, we may now be able to better investigate the mechanisms of neural dysfunction and recovery. In order to understand the significance of the hypoperfusion observed after TBI, it is helpful to return to the question of the relationship between structural pathology and perfusion. To do so, one must consider the effects of both focal and diffuse structural pathology on both local and remote perfusion. As mentioned previously, it is not surprising that hypoperfusion in areas of focal cortical injury was seen, representing the local effects of focal loss of tissue and its associated perfusion. But no additional areas of hypoperfusion outside focally-lesioned areas were seen in the focal injury group that were not also present in the diffuse group, as demonstrated by the direct comparison of the two subgroups. Does this mean that focal lesions in chronic TBI do not have distal effects on the neural function (and associated perfusion demand) of remote areas? One possibility is that the distal effects of focal lesions on perfusion (i.e., diaschisis) are only present in the relatively acute phase, and have largely resolved by the time these participants were studied, a mean of more than 5 years post-injury. Alternatively, individuals may vary in the topography of the distal effects on CBF, or these effects may simply be smaller in magnitude, such that the current study lacked sufficient power to detect them. Thus, future studies that attempt to quantify the individualized effects of focal structural lesions on cortical areas with known interconnections to those areas are warranted, along with studies conducted earlier after injury.

Several limitations of the current study should be noted. First, we only had partial coverage of the cerebellum. Thus, the lack of significant CBF reductions seen in cerebellum in our results should be interpreted with caution. This is espe-

cially true given the fact that the cerebellum is known to be vulnerable to diaschisis due to its connection to the frontal cortices (Sasaki et al., 1979; Schmahmann and Pandya, 1997). Second, the requirement of a complaint of attention difficulties may limit the generalizability of the results; however, attention deficits are exceedingly common after TBI (Ponsford and Kinsella, 1992), so this is by no means a highly selected sample. Third, since the overall sample size was relatively small, and the sizes used for the subgroup analyses were smaller still, the areas of significant hypoperfusion likely represent simply the most seriously affected regions, and additional areas would likely be identified in larger studies. In particular, the subgroup analysis is certainly under-powered, and appropriate caution should be applied in interpreting the results. To the extent that neural depression caused by structural pathology elsewhere may produce milder hypoperfusion than frank loss of tissue, this study may have been less sensitive to these remote effects. Fourth, this study was cross-sectional in nature, and conducted for the most part long after injury, which may account for the fact that little evidence of functional depression remote from areas of structural pathology was found. It is likely that longitudinal studies that begin sooner after injury might enhance the understanding of the relationship between structural pathology and functional depression, since these phenomena likely play out over different time courses. Finally, these data were collected from individuals with moderate to severe injuries, and cannot be generalized to those with milder injuries, who typically lack focal pathology. One might speculate that their pattern of diffuse damage would be similar to that of the diffuse subgroup in this study but smaller in magnitude, but this remains to be assessed.

Acknowledgments

Author Disclosure Statement

No competing financial interests exist.

Dr. Detre is an inventor on the University of Pennsylvania's patent for ASL MRI and is entitled to institutional royalty sharing for its licensure.

References

Ances, B.M., Zarahn, E., Greenberg, J.H., and Detre, J.A. (2000). Coupling of neural activation to blood flow in the somatosensory cortex of rats is time-intensity separable, but not linear. J. Cereb. Blood Flow Metab. 20, 921–930.

Anderson, K.E., Taber, K.H., and Hurley, R.A. (2005). Functional imaging, in: *Textbook of Traumatic Brain Injury*. J.M. Silver, T.W. McAllister, and S.C. Yudofsky (eds), American Psychiatric Publishing: Washington DC, pps. 107–133.

Avants, B., and Gee, J.C. (2004). Geodesic estimation for large deformation anatomical shape averaging and interpolation. Neuroimage 23(Suppl. 1), S139–S150.

Avants, B., Epstein, C.L., Grossman, M., and Gee, J.C. (2008). Symmetric diffeomorphic image registration with cross-correlation: evaluating automated labeling of elderly and neurodegenerative brain. Med. Image Anal. 12, 26–41.

Azouvi, P. (2000). Neuroimaging correlates of cognitive and functional outcome after traumatic brain injury. Curr. Opin. Neurol. 13, 665–669.

Borghammer, P., Cumming, P., Aanerud, J., and Gjedde, A. (2009a). Artefactual subcortical hyperperfusion in PET studies normalized to global mean: lessons from Parkinson's disease. Neuroimage 45, 249–257.

Borghammer, P., Cumming, P., Aanerud, J., Forster, S., and Gjedde, A. (2009b). Subcortical elevation of metabolism in Parkinson's disease—a critical reappraisal in the context of global mean normalization. Neuroimage 47, 1514–1521.

Brett, M., Leff, A.P., Rorden, C., and Ashburner, J. (2001). Spatial normalization of brain images with focal lesions using cost function masking. Neuroimage 14, 486–500.

Casanova, R., Srikanth, R., Baer, A., Laurienti, P.J., Burdette, J.H., Hayasaka, S., Flowers, L., Wood, F., and Maldjian, J.A. (2007). Biological parametric mapping: A statistical toolbox for multimodality brain image analysis. Neuroimage 34, 137–143.

Chiu Wong, S.B., Chapman, S.B., Cook, L.G., Anand, R., Gamino, J.F., and Devous, M.D., Sr. (2006). A SPECT study of language and brain reorganization three years after pediatric brain injury. Prog. Brain Res. 157, 173–185.

Detre, J.A., and Wang, J. (2002). Technical aspects and utility of fMRI using BOLD and ASL. Clin. Neurophysiol. 113, 621–634.

Fransson, P., and Marrelec, G. (2008). The precuneus/posterior cingulate cortex plays a pivotal role in the default mode network: Evidence from a partial correlation network analysis. Neuroimage 42, 1178–1184.

Goldenberg, G., Oder, W., Spatt, J., and Podreka, I. (1992). Cerebral correlates of disturbed executive function and memory in survivors of severe closed head injury: a SPECT study. J. Neurol. Neurosurg. Psychiatry 55, 362–368.

Greicius, M.D., Srivastava, G., Reiss, A.L., and Menon, V. (2004). Default-mode network activity distinguishes Alzheimer's disease from healthy aging: evidence from functional MRI. Proc. Natl. Acad. Sci. USA 101, 4637–4642.

Grunder, G. (2009). "Absolute" or "relative": choosing the right outcome measure in neuroimaging. Neuroimage 45, 258–259.

Hattori, N., Huang, S.C., Wu, H.M., Liao, W., Glenn, T.C., Vespa, P.M., Phelps, M.E., Hovda, D.A., and Bergsneider, M. (2003). PET investigation of post-traumatic cerebral blood volume and blood flow. Acta Neurochir. Suppl. 86, 49–52.

Himanen, L., Portin, R., Isoniemi, H., Helenius, H., Kurki, T., and Tenovuo, O. (2006). Longitudinal cognitive changes in traumatic brain injury: a 30-year follow-up study. Neurology 66, 187–192.

Ichise, M., Chung, D.G., Wang, P., Wortzman, G., Gray, B.G., and Franks, W. (1994). Technetium-99m-HMPAO SPECT, CT and MRI in the evaluation of patients with chronic traumatic brain injury: a correlation with neuropsychological performance. J. Nucl. Med. 35, 217–226.

Inoue, Y., Shiozaki, T., Tasaki, O., Hayakata, T., Ikegawa, H., Yoshiya, K., Fujinaka, T., Tanaka, H., Shimazu, T., and

Sugimoto, H. (2005). Changes in cerebral blood flow from the acute to the chronic phase of severe head injury. J. Neurotrauma 22, 1411–1418.

Jennett, B., Snoek, J., Bond, M.R., and Brooks, N. (1981). Disability after severe head injury: observations on the use of the Glasgow Outcome Scale. J. Neurol. Neurosurg. Psychiatry 44, 285–293.

Kato, T., Nakayama, N., Yasokawa, Y., Okumura, A., Shinoda, J., and Iwama, T. (2007). Statistical image analysis of cerebral glucose metabolism in patients with cognitive impairment following diffuse traumatic brain injury. J. Neurotrauma 24, 919–926.

Kelly, A.M., Uddin, L.Q., Biswal, B.B., Castellanos, F.X., and Milham, M.P. (2008). Competition between functional brain networks mediates behavioral variability. Neuroimage 39, 527–537.

Kim, E., Ku, J., Namkoong, K., Lee, W., Lee, K.S., Park, J.Y., Lee, S.Y., Kim, J.J., Kim, S.I., and Jung, Y.C. (2009). Mammillothalamic functional connectivity and memory function in Wernicke's encephalopathy. Brain 132, 369–376.

Kim, J., Avants, B., Patel, S., Whyte, J., Coslett, B.H., Pluta, J., Detre, J.A., & Gee, J.C. (2008). Structural consequences of diffuse traumatic brain injury: A large deformation tensor-based morphometry study. Neuroimage 39, 1014–1026.

Kim, J., Whyte, J., Wang, J., Rao, H., Tang, K.Z., and Detre, J.A. (2006). Continuous ASL perfusion fMRI investigation of higher cognition: quantification of tonic CBF changes during sustained attention and working memory tasks. Neuroimage 31, 376–385.

Kochanek, P.M., Hendrich, K.S., Dixon, C.E., Schiding, J.K., Williams, D.S., and Ho, C. (2002). Cerebral blood flow at one year after controlled cortical impact in rats: assessment by magnetic resonance imaging. J. Neurotrauma 19, 1029–1037.

Kogure, D., Matsuda, H., Ohnishi, T., Asada, T., Uno, M., Kunihiro, T., Nakano, S., and Takasaki, M. (2000). Longitudinal evaluation of early Alzheimer's disease using brain perfusion SPECT. J. Nucl. Med. 41, 1155–1162.

Lannoo, E., Colardyn, F., Jannes, C., and de Soete, G. (2001). Course of neuropsychological recovery from moderate-to-severe head injury: a 2-year follow-up. Brain Inj. 15, 1–13.

Lifshitz, J., Kelley, B.J., and Povlishock, J.T. (2007). Perisomatic thalamic axotomy after diffuse traumatic brain injury is associated with atrophy rather than cell death. J. Neuropathol. Exp. Neurol. 66, 218–229.

Mai, J.K., Assheuer, J.K., and Paxinos, G. (2004). Atlas of the Human Brain, 2nd ed. Academic Press: San Diego.

Millis, S.R., Rosenthal, M., Novack, T.A., Sherer, M., Nick, T.G., Kreutzer, J.S., High, W.M., Jr., and Ricker, J.H. (2001). Long-term neuropsychological outcome after traumatic brain injury. J. Head Trauma Rehabil. 16, 343–355.

Nakashima, T., Nakayama, N., Miwa, K., Okumura, A., Soeda, A., and Iwama, T. (2007). Focal brain glucose hypometabolism in patients with neuropsychologic deficits after diffuse axonal injury. AJNR Am. J. Neuroradiol. 28, 236–242.

Ngai, A.C., Ko, K.R., Morii, S., and Winn, H.R. (1988). Effect of sciatic nerve stimulation on pial arterioles in rats. Am. J. Physiol. 254, H133–H139.

Oder, W., Goldenberg, G., Spatt, J., Podreka, I., Binder, H., and Deecke, L. (1992). Behavioural and psychosocial sequelae of severe closed head injury and regional cerebral blood flow: a SPECT study. J. Neurol. Neurosurg. Psychiatry, 55, 475–480.

Perlstein, W.M., Cole, M.A., Demery, J.A., Seignourel, P.J., Dixit, N.K., Larson, M.J., and Briggs, R.W. (2004). Parametric manipulation of working memory load in traumatic brain injury: behavioral and neural correlates. J. Int. Neuropsychol. Soc. 10, 724–741.

Ponsford, J., and Kinsella, G. (1992). Attentional deficits following closed-head injury. J. Clin. Exp. Neuropsychol. 14, 822–838.

Prayer, L., Wimberger, D., Oder, W., Kramer, J., Schindler, E., Podreka, I., and Imhof, H. (1993). Cranial MR imaging and cerebral 99mTc HM-PAO-SPECT in patients with subacute or chronic severe closed head injury and normal CT examinations. Acta Radiol. 34, 593–599.

Rao, H., Wang, J., Tang, K., Pan, W., and Detre, J.A. (2007). Imaging brain activity during natural vision using CASL perfusion fMRI. Hum. Brain Mapp. 28, 593–601.

Ricker, J.H., Hillary, F.G., and DeLuca, J. (2001). Functionally activated brain imaging (O-15 PET and fMRI) in the study of learning and memory after traumatic brain injury. J. Head Trauma Rehabil. 16, 191–205.

Rombouts, S.A., Barkhof, F., Goekoop, R., Stam, C.J., and Scheltens, P. (2005). Altered resting state networks in mild cognitive impairment and mild Alzheimer's disease: an fMRI study. Hum. Brain Mapp. 26, 231–239.

Rutland-Brown, W., Langlois, J.A., Thomas, K.E., and Xi, Y.L. (2006). Incidence of traumatic brain injury in the United States, 2003. J. Head Trauma Rehabil. 21, 544–548.

Sanchez-Carrion, R., Gomez, P.V., Junque, C., Fernandez-Espejo, D., Falcon, C., Bargallo, N., Roig-Rovira, T., Ensenat-Cantallops, A., and Bernabeu, M. (2008). Frontal hypoactivation on functional magnetic resonance imaging in working memory after severe diffuse traumatic brain injury. J. Neurotrauma 25, 479–494.

Sasaki, K., Jinnai, K., Gemba, H., Hashimoto, S., and Mizuno, N. (1979). Projection of the cerebellar dentate nucleus onto the frontal association cortex in monkeys. Exp. Brain Res. 37, 193–198.

Schmahmann, J.D., and Pandya, D.N. (1997). Anatomic organization of the basilar pontine projections from prefrontal cortices in rhesus monkey. J. Neurosci. 17, 438–458.

Schwartz, M.F., Brecher, A.R., Whyte, J., and Klein, M.G. (2005). A patient registry for cognitive rehabilitation research: a strategy for balancing patients' privacy rights with researchers' need for access. Arch. Phys. Med. Rehabil. 86, 1807–1814.

Shin, Y.B., Kim, S.J., Kim, I.J., Kim, Y.K., Kim, D.S., Park, J.H., and Yeom, S.R. (2006). Voxel-based statistical analysis of cerebral blood flow using Tc-99m ECD brain SPECT in patients with traumatic brain injury: group and individual analyses. Brain Inj. 20, 661–667.

Stamatakis, E.A., Wilson, J.T., Hadley, D.M., and Wyper, D.J. (2002). SPECT imaging in head injury interpreted with statistical parametric mapping. J. Nucl. Med. 43, 476–483.

Strangman, G., O'Neil-Pirozzi, T.M., Burke, D., Cristina, D., Goldstein, R., Rauch, S.L., Savage, C.R., and Glenn, M.B. (2005). Functional neuroimaging and cognitive rehabilitation for people with traumatic brain injury. Am. J. Phys. Med. Rehabil. 84, 62–75.

Thurman, D.J., Alverson, C., Dunn, K.A., Guerrero, J., and Sniezek, J.E. (1999). Traumatic brain injury in the United States: A public health perspective. J. Head Trauma Rehabil. 14, 602–615.

Troiani, V., Fernandez-Seara, M.A., Wang, Z., Detre, J.A., Ash, S., and Grossman, M. (2008). Narrative speech production: an fMRI study using continuous arterial spin labeling. Neuroimage 40, 932–939.

Vanhaudenhuyse, A., Noirhomme, Q., Tshibanda, L.J., Bruno, M.A., Boveroux, P., Schnakers, C., Soddu, A., Perlbarg, V.,

Ledoux, D., Brichant, J.F., Moonen, G., Maquet, P., Greicius, M.D., Laureys, S., and Boly, M. (2010). Default network connectivity reflects the level of consciousness in non-communicative brain-damaged patients. Brain 133, 161–171.

Wang, J., Zhang, Y., Wolf, R.L., Roc, A.C., Alsop, D.C., and Detre, J.A. (2005). Amplitude-modulated continuous arterial spin-labeling 3.0-T perfusion MR imaging with a single coil: feasibility study. Radiology 235, 218–228.

Weissman, D., Roberts, K.C., Visscher, K.M., and Woldorff, M.G. (2006). The neural bases of momentary lapses in attention. Nat. Neurosci. 9, 971–978.

Werner, C., and Engelhard, K. (2007). Pathophysiology of traumatic brain injury. Br. J. Anaesth. 99, 4–9.

Wolf, R. L., and Detre, J.A. (2007). Clinical neuroimaging using arterial spin-labeled perfusion magnetic resonance imaging. Neurotherapeutics 4, 346–359.

Address correspondence to:
Junghoon Kim, Ph.D.
Moss Rehabilitation Research Institute
Albert Einstein Healthcare Network
60 Township Line Road
Elkins Park, PA 19027

E-mail: kimj@einstein.edu